

BBAMEM 75979

## Sodium/proton transport by apical membranes of type-II pneumocytes

David G. Oelberg, Fang Xu and Faten Shabarek

*Department of Pediatrics, University of Texas Health Science Center at Houston, Houston, TX (USA)*

(Received 1 October 1992)

(Revised manuscript received 22 January 1993)

**Key words:** Sodium ion channel; Sodium ion–proton exchange; Plasma membrane vesicle

Recent studies fail to confirm the coexistence of  $\text{Na}^+$  channels and  $\text{Na}^+/\text{H}^+$  exchange at the apical membranes of lower airway epithelia. Availability of plasma membrane vesicles simplifies the investigation of membrane transport processes. Apical and basolateral plasma membrane vesicles of disrupted type-II pneumocytes were fractionated upon nonlinear, continuous sucrose gradients. To investigate sodium transport,  $^{22}\text{Na}^+$  uptake by apical membrane vesicles was assayed in the presence and absence of transmembrane sodium diffusion potentials. Interior-negative sodium diffusion potentials promoted  $^{22}\text{Na}^+$  uptake 1.5-fold. Internally-directed  $\text{H}^+$  gradients or  $\text{NH}_4^+$  gradients inhibited  $^{22}\text{Na}^+$  uptake 40–50%. Amiloride (1–1000  $\mu\text{M}$ ) inhibited uptake 10–79%. To investigate  $\text{H}^+$  transport, decay of transmembrane pH gradients was monitored with pH probe acridine orange. In the presence or absence of externally-directed  $\text{H}^+$  gradients, external sodium promoted internal alkalinization, except in the presence of external amiloride. These observations of amiloride-sensitive, electrogenic  $\text{Na}^+$  uptake and amiloride-sensitive, electroneutral,  $\text{Na}^+/\text{H}^+$  coupling indicate coexistence of  $\text{Na}^+$  channels and  $\text{Na}^+/\text{H}^+$  exchange at the apical membrane of type-II pneumocytes.

### Introduction

Effective gas exchange across lower airway epithelia depends upon efficient salt and water transport between alveolar and interstitial spaces. Alveoli are kept dry by the active reabsorption of sodium across the apical side of type-II pneumocytes (TIIPs) [1–3]. Despite interest in the mechanisms underlying these important transport activities, investigations have been hampered by the inaccessibility of alveolar epithelia to *in vivo* investigation.

Studies of confluent monolayers have shed considerable light on the vectorial movement of salts. These studies support the presence of ouabain-sensitive  $\text{Na}^+/\text{K}^+$ -ATPase at the basolateral membrane [4]. Hydrolysis of ATP by  $\text{Na}^+/\text{K}^+$ -ATPase energizes extrusion of  $\text{Na}^+$  from cells in exchange for  $\text{K}^+$  that establishes an electrochemical gradient favorable for  $\text{Na}^+$ -coupled or secondary active transport of other ions. Inhibition of  $\text{Na}^+/\text{K}^+$ -ATPase by ouabain blocks  $\text{Rb}^+$

uptake by isolated, intact TIIPs [5]; inhibits dome formation – believed to result from active transport of ions from the apical to basolateral surface of confluent monolayers [1]; and inhibits the short circuit current or transepithelial potential difference across confluent monolayers when applied to the basolateral side [4]. Evidence for active  $\text{Na}^+$  transport by TIIPs is provided by the dependence of dome formation and short-circuit currents upon extracellular  $\text{Na}^+$  presence.

Reports of inhibited dome formation and short-circuit currents by amiloride suggest two paths of  $\text{Na}^+$  absorption by TIIPs. At micromolar concentrations, amiloride inhibits  $\text{Na}^+$  channels in epithelia [6]. By the accepted model,  $\text{Na}^+$  enters cells by  $\text{Na}^+$  channels at the apical membrane and exits by  $\text{Na}^+/\text{K}^+$ -ATPase at the basolateral membrane. At somewhat higher concentrations amiloride also inhibits  $\text{Na}^+/\text{H}^+$  exchange [6]. In lungs, observations of reduced pH at aqueous alveolar subphases and of  $\text{Na}^+$ -dependent, amiloride-sensitive alkalinization of intact TIIPs support the presence of  $\text{Na}^+/\text{H}^+$  exchange [7,8]. By contrast, evidence of  $\text{Na}^+/\text{H}^+$  exchange by apical membranes prepared from TIIPs is conflicting. In apical membranes prepared from fetal sheep TIIPs, outwardly-directed proton gradients stimulate amiloride-sensitive  $\text{Na}^+$  up-

Correspondence to: D. Oelberg, Department of Pediatrics, University of Texas Medical School, 6431 Fannin, MSB 3.256, Houston, TX 77030, USA.

take [9,10]. This is interpreted as evidence for the exchange mechanism. In another preparation of mixed plasma membrane vesicles, experiments favor an electrogenic path of  $\text{Na}^+$  entry [11]. By analogy with other polarized epithelia, it is probable that  $\text{Na}^+$  channels and  $\text{Na}^+/\text{H}^+$  exchange coexist on the apical membrane. Nevertheless, direct evidence of coexistence in an experimental preparation of intact TIIPs or plasma-membrane vesicles is lacking.

Examination of complex transport pathways employing fractionated plasma membranes offers several advantages. They include isolation of apical from basolateral activities, isolation of membrane activities from cytoplasmic activities, manipulation of intra- and extra-vesicular fluid composition for analysis of driving forces, investigation of kinetic and biochemical properties of membrane-bound transport systems and avoidance of cell dedifferentiation that may otherwise occur in cultured systems.

The purpose of this investigation was to develop a technique for isolating fractions of plasma membrane vesicles from TIIPs, enriched in enzyme markers for apical and basolateral membranes. It was believed that physical separation of apical from basolateral plasma membranes would permit investigation of complex interdependent  $\text{Na}^+$  transport mechanisms. Initial investigations examine the possible coexistence of  $\text{Na}^+$  channels and  $\text{Na}^+/\text{H}^+$  exchangers at the apical membrane.

## Materials and Methods

*Isolation of type-II pneumocytes.* The method of type-II pneumocyte isolation was adapted from that of Augustin-Voss et al. [12]. Adult bovine lungs were obtained from a local abattoir. A segmental section was isolated (150–200 g), the secondary bronchus was cannulated, and the associated pulmonary artery was perfused with phosphate-buffered saline until drainage cleared. Minimal essential medium (MEM) with trypsin (1:250, 5 mg/ml (pH 7.4), 37°C) followed by 100 ml air were infused in bronchus, cannula was sealed, and the inflated tissue incubated (37°C, 1 h). The segment was minced in a Waring Commercial Blender (Waring, New Hartford, CT, USA), stirred (30 min, 37°C) and filtered through cotton gauze. Free cells in the filtrate were defibrinated by addition of 100–200 glass beads with slow stirring for 3 periods (10 min, 25°C) [12]. The defibrinated cell suspension was filtered through nylon mesh (52  $\mu$  opening, 70  $\mu$  thickness; Spectrum Medical, Los Angeles, CA, USA) and brought to a final volume of 1 l with cold MEM plus 10% calf serum. Subsequently, all cell preparations were maintained at 1–4°C. Cells were pelleted (600  $\times g$  for 15 min), resuspended in erythrocyte lysing solution (155 mM  $\text{NH}_4\text{Cl}$ , 10 mM Tris-HCl (pH 7.4)), diluted with MEM and

repelleted. Cells were resuspended in small volumes of erythrocyte lysing solution plus DNAase (10 mg/ml) and layered on top of preformed Percoll gradients (20.3:14.7 (v/v) iso-osmotic Percoll/MEM – 20 500  $\times g$  for 20 min) for separation by density gradient centrifugation (800  $\times g$  for 60 min). The upper cell layers with densities less than 1.050 g/ml were washed with MEM plus DNAase, pelleted, and suspended in homogenization buffer (250 mM mannitol, 0.2 mM  $\text{CaCl}_2$ , 0.2 mM  $\text{MgCl}_2$ , 5 mM Tris-Hepes (pH 7.4), 1 mM dithiothreitol). Cell viability was estimated by exclusion of Trypan blue dye from the cytoplasm during cell counts employing a hemocytometer. Cell smears were prepared and stained by a modified Papanicolaou technique to differentiate TIIPs from other cell types [13].

*Preparation and purification of plasma membrane vesicles.* Cells were disrupted in a nitrogen cavitation bomb (Parr Instrument, Moline, IL, USA) at 800 psi for 2  $\times$  15 min. Undisrupted cells and denser cell organelles were pelleted (600  $\times g$  for 10 min). The remaining cell particles were pelleted from the supernatant (48 000  $\times g$  for 60 min). The pelleted particles were resuspended in 2 ml of homogenization buffer, layered on a 12.5–50% nonlinear, continuous sucrose gradient, and centrifuged at 75 000  $\times g$  for 4 h in a Beckman SW-27 ultracentrifuge rotor. The gradient was fractionated by upward displacement with 40% NaBr. Fractions were washed, pelleted and resuspended in 2–4 ml homogenization buffer.

*Enzyme assays.* Fractions were characterized by the presence of standard enzyme markers for plasma membranes, mitochondria, endoplasmic reticulum and nuclei. Alkaline phosphatase and  $\text{Na}^+, \text{K}^+$ -ATPase were chosen as specific markers for apical and basolateral plasma membranes, respectively. Alkaline phosphatase activity was assayed by the method of Langridge-Smith et al. at 37°C [14]. A modification of the coupled ATPase assay of Norby was used to measure  $\text{Na}^+, \text{K}^+$ -ATPase activity [15]. Fraction samples were solubilized with 0.1% polyoxyethylene ether W-1 in a medium of 120 mM NaCl, 20 mM KCl, 20 mM histidine, 20 mM  $\text{MgCl}_2$  and 2 mM EGTA (pH 7.4). The assay was initiated by addition of a stock solution providing final concentrations of 3 mM ATP, 3 mM phosphoenolpyruvate, 0.1 mM NADH, 2 U/ml pyruvate kinase and 10 U/ml lactate dehydrogenase. Oxidation of NADH was monitored by the change in absorbance at 340 nm in a thermostatted cuvette compartment (37°C).  $\text{Na}^+, \text{K}^+$ -ATPase activity was determined through the difference between total and ouabain-insensitive ATPase activities in the absence and presence of 2 mM ouabain, respectively. Succinic dehydrogenase and NADH dehydrogenase activities, markers for mitochondria and endoplasmic reticulum, respectively, were assayed by methods of Hochstadt et al. [16]. Nuclear DNA was measured by the method of Labarca and Paigen em-

ploying fluorescent dye Hoechst H 33258 [17]. Protein was estimated with standards of bovine serum albumin by the method of Lowry et al. [18].

**<sup>22</sup>Na transport assays.** Sodium transport by apical vesicles was assessed by net uptake measurements of radioactive <sup>22</sup>Na<sup>+</sup>. Fractions of plasma membrane vesicles enriched at least 4-fold in apical enzyme markers and contaminated less than 2-fold by other enzyme markers were loaded with two different internal environments. For the first internal environment, vesicles were loaded with nonradioactive NaCl by incubating vesicles at 2°C with 20 volumes of buffer containing 55 mM NaCl, 87.5 mM mannitol, 12.5 mM Tris-Hepes (pH 7.0) and 2.5 mM EDTA for 4 h. To substitute mannitol for NaCl, 175 mM mannitol and 5 mM Tris-Hepes (pH 7.0) were present in the second internal environment. After loading with either environment, vesicles were pelleted (48 000 × g for 60 min), resuspended in the mannitol or NaCl buffer at protein concentrations of about 1 mg/ml and frozen at -70°C until use.

Immediately prior to assay, aliquots of mannitol- or NaCl-loaded vesicles were thawed. Sodium-loaded vesicles were eluted through a Dowex cation exchange column to remove external Na<sup>+</sup>. This procedure created transient, transmembrane, inside-negative, electrical diffusion potentials favoring electrogenic uptake of cations by NaCl-loaded vesicles [19]. Cation exchange columns (0.5 × 7.5 cm) were prepared by the method of Gasko et al. by pouring 1.5 ml of Dowex 50W-X8, 50–100 mesh, Tris<sup>+</sup> form into a Pasteur pipette with a dacron wool plug [20]. Vesicles were eluted from the column with 7 × 200 μl aliquots of 175 mM mannitol, 5 mM Tris-Hepes (pH 7.0) at 2°C. Mannitol-loaded vesicles or eluted Na<sup>+</sup>-loaded vesicles were diluted with 1.4 ml 175 mM mannitol, 5 mM Tris-Hepes (pH 7.0). For some experiments, Na<sup>+</sup>-loaded vesicles were diluted with 1.4 ml 110 mM NaCl, 5 mM Tris-Hepes (pH 7.0). For others, amiloride (1.0 μM–1.0 mM) was present in the diluent. External mannitol pH values were decreased from 7 to 6 in experimental protocols employing Na<sup>+</sup>-loaded vesicles. In separate experiments, effects of external medium osmolarity upon <sup>22</sup>Na<sup>+</sup> uptake by Na<sup>+</sup>-loaded vesicles were examined at final mannitol concentrations decreasing from 500 mM to 125 mM.

Transport studies were conducted at 2°C. Within 15 s of vesicle dilution by mannitol or NaCl buffer, the uptake of <sup>22</sup>Na<sup>+</sup> was initiated by addition of 3 μCi of <sup>22</sup>NaCl (New England Nuclear, Boston, MA, USA; spec. act. 47.7 mCi/mmol). At 0 min and subsequent timepoints of 1, 2, 5, 10 and 60 min, aliquots (400 μl) of the vesicle-containing reaction mixture were applied to Dowex cation-exchange columns for removal of external <sup>22</sup>Na<sup>+</sup>. Vesicles containing trapped <sup>22</sup>Na<sup>+</sup> cations were eluted from the column with 1.4 ml × 2 of

175 mM mannitol. Elution times for the vesicles were less than 20 s. Eluents were collected, and radiolabelled contents were analyzed in a Cobra 5000 Series Auto-Gamma Counting System (Packard Instruments, Downers Grove, IL, USA). Uptake of <sup>22</sup>Na<sup>+</sup> was expressed as fractions of initial total radioactivity per mg of vesicle protein.

**Determination of ΔpH changes.** Changes in transmembrane pH gradients were spectrophotometrically monitored by acridine orange (AO) trapping in the intravesicular compartment. AO trapping, indicated by absorbance at 492 nm, decreased as intravesicular pH increased relative to the extravesicular environment [21]. Apical vesicles (1 mg protein/ml) loaded with either 175 mM mannitol, 5 mM Tris-Hepes (pH 6.0 or 7.0) (buffer A) or 55 mM NaCl, 87.5 mM mannitol, 5 mM Tris-Hepes (pH 6.0 or 7.0) (buffer B) were prewarmed to 37°C. Experiments were initiated by addition of vesicles to a thermostatted cuvette (37°C) with 6 μM AO in either buffer A (pH 7.0) or buffer B (pH 7.0). Relative ΔpH change was monitored over time as the difference between absorbances (ΔA<sub>492 nm</sub>) before and after the addition of vesicles. An increase in ΔA<sub>492 nm</sub> indicated intravesicular alkalinization relative to the extravesicular compartment.

**Statistical analyses.** Data were described by the mean ± S.E. unless otherwise indicated. Comparative analyses of <sup>22</sup>Na<sup>+</sup> uptake over time with and without amiloride at pH values of 6 and 7 were conducted by two-way analysis of variance with repeated measures. Post hoc comparisons were accomplished by the Newman-Keuls multiple range test. Differences were considered statistically significant if *P* < 0.05. Linear regression analysis was performed by the least-squares method.

**Materials.** Trypsin was obtained from Gibco Laboratories (Grand Island, NY, USA). Tris base and Hoechst dye H 33258 were available from Boehringer-Mannheim (Indianapolis, IN, USA). Calf serum was purchased from Hazelton Research Products (Denver, PA, USA). Other chemicals, drugs, enzymes, culture media and cation-exchange resin were available from Sigma (St. Louis, MO, USA).

## Results

### *Isolation and characterization of plasma membrane fractions*

Preparation of plasma membrane fractions began with isolation of (10–25) · 10<sup>9</sup> cells from adult bovine lung tissue, of which 90% or greater were TIIPs. Cell viability averaged 90–95%. Early low-speed centrifugation (600 × g) of homogenized cells provided a pellet enriched in nuclei, mitochondria and endoplasmic reticulum (Table I). Subsequent separation of the supernatant on a continuous sucrose gradient provided

TABLE I

*Mean recoveries and yields of biochemical markers during isolation of plasma membrane vesicles from bovine type-II pneumocytes*

Mean values were calculated from 24 experimental preparations performed over a 10-months period. Yields are expressed as percentages of the total homogenate values. Enzyme activities for alkaline phosphatase and  $\text{Na}^+/\text{K}^+$ -ATPase are expressed as  $\mu\text{mol}$  of inorganic phosphate produced/h per mg protein. Enzyme activities for succinate dehydrogenase and NADH dehydrogenase are expressed as  $\mu\text{mol}$  of substrate oxidized/h per mg protein. Fractions: H, homogenate after cell disruption by nitrogen cavitation; P, pellet after low-speed centrifugation of the homogenate; MMF, mixed fraction of cellular particles after pellet removal; BL, combined fractions of the sucrose gradient enriched in basolateral membrane marker  $\text{Na}^+/\text{K}^+$ -ATPase; AP, combined fractions of the sucrose gradient enriched in apical membrane marker alkaline phosphatase.

Fraction	Protein		DNA		Alkaline phosphatase			Na <sup>+</sup> , K <sup>+</sup> -ATPase			Succinate dehydrogenase			NADH dehydrogenase		
	total mg	yield	total mg	yield	total act	spec act	yield	total act	spec act	yield	total act	spec act	yield	total act	spec act	yield
H	232	100	974	100	650	2.79	100	115	0.49	100	1338	5.76	100	8975	38.59	100
P	38	16	867	89	139	0.91	21	28	0.18	24	129	3.39	15	2833	18.51	32
MF	196	84	88	9	602	3.36	93	54	0.27	47	1050	3.54	78	5784	29.33	64
BL	3	1	4	<1	16	5.24	2	35	11.22	30	2	1.53	<1	44	27.79	<1
AP	11	5	9	<1	57	14.24	9	9	0.87	8	88	7.12	7	314	58.91	3

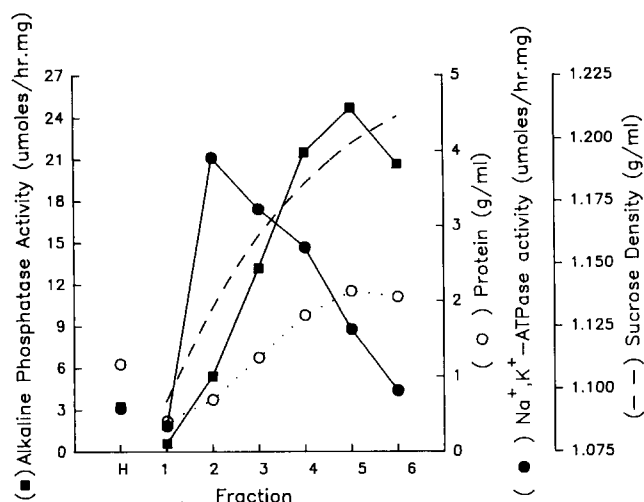


Fig. 1. Distribution of enzyme markers for apical and basolateral membranes on the continuous sucrose gradient. Homogenate (H) and fractions 1–6 are indicated on the abscissa. Ordinate axes from left to right indicate: mean specific activity for apical membrane marker alkaline phosphatase (■); mean protein concentration (○) and mean specific activity for basolateral membrane marker  $\text{Na}^+, \text{K}^+$ -ATPase (●) and sucrose gradient density profile (broken curve).

fractions enriched with enzyme markers for apical and basolateral plasma membranes (Fig. 1).  $\text{Na}^+, \text{K}^+$ -ATPase activities were greatest for fractions 2, 3 and 4. These fractions were isolated at densities of 1.130–1.155 on the continuous, nonlinear sucrose gradient. Alkaline phosphatase activities were greatest in fractions 4, 5 and 6, corresponding to gradient densities of 1.155–1.210. During each preparation, the individual fractions providing the greatest  $\text{Na}^+, \text{K}^+$ -ATPase or alkaline phosphatase specific activity with least contamination by other enzyme markers were identified as ‘basolateral’ and ‘apical’ fractions, respectively. On the average, basolateral fractions were enriched 23-fold in  $\text{Na}^+, \text{K}^+$ -ATPase activity with minimal contamination by other enzyme markers (Table I). All ouabain-sensitive ATPase activity disappeared within 3–4 days of vesicle preparation. An average 28% of total  $\text{Na}^+, \text{K}^+$ -ATPase activity was recovered in the basolateral fraction. Similarly, apical fractions were enriched 5-fold in alkaline phosphatase activity with little contamination by other organelles. 9% of total alkaline phosphatase activity was recovered in the enriched apical membrane fractions. As expected, all enzyme activities were abolished by membrane freezing.

#### Evidence for electrogenic sodium uptake by apical vesicles

$\text{Na}^+$  uptake into an osmotically-active space was demonstrated by monitoring uptake across a range of external osmolarities. External osmolarity was varied from 500 to 125 mM. Fig. 2 displays the inverse linear relationship between osmolarity and  $^{22}\text{Na}^+$  uptake by

apical vesicles after 60 min ( $r = 0.93$ ). Extrapolation of the  $^{22}\text{Na}^+$  uptake regression line to infinite osmolarity – the point at which osmotically-active intravesicular spaces disappear – provided an estimate of  $^{22}\text{Na}^+$  binding to vesicle membranes. By this estimation  $0.89 \pm 0.34\%$  (95% confidence interval) of total radioactivity per mg protein was bound to membrane. Disruption of intravesicular spaces with detergent Triton X-100 (0.5%) provided an alternative binding estimate of  $0.59 \pm 0.14\%$  total radioactivity/mg protein (Fig. 2). By these estimations of  $^{22}\text{Na}^+$  binding to apical membranes, approx. 25% of final  $^{22}\text{Na}^+$  uptake was attributable to membrane binding or adsorption.

Vesicles exhibited time-dependent  $^{22}\text{Na}^+$  uptake in the presence and absence of imposed  $\text{Na}^+$  potential gradients. Fig. 3 indicates the time-courses of  $^{22}\text{Na}^+$  uptake by apical vesicles in three different ionic environments. Within each environment, uptake significantly progressed over the 60-min period of observation ( $P < 0.01$ ). Approx. 75% of the final uptake at 60 min occurred within the first 10 min of study.  $^{22}\text{Na}^+$  uptake was greatest in the presence of an imposed diffusion potential gradient created by elution of sodium-loaded vesicles through cation-exchange columns and incubation of eluted vesicles in mannitol prior to  $^{22}\text{NaCl}$  addition ( $\text{Na}_{\text{Int}}^+/\text{Mtl}_{\text{Ext}}$ ) ( $P < 0.01$ ).

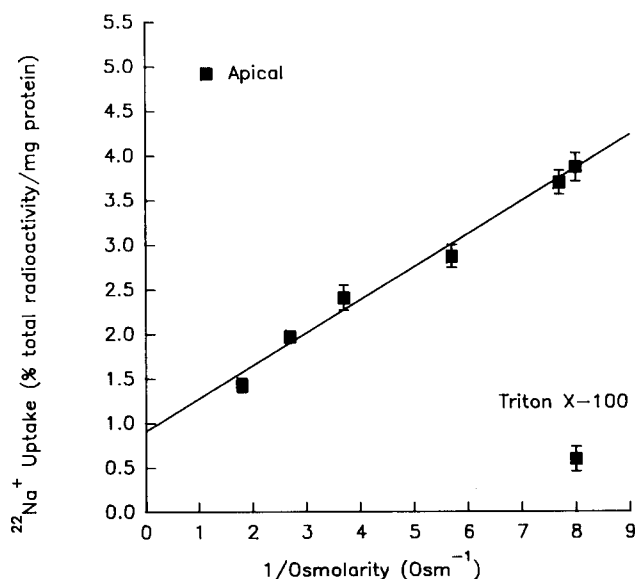


Fig. 2.  $^{22}\text{Na}^+$  uptake by apical membrane vesicles as a function of extravesicular osmolarity. Apical vesicles loaded with 55 mM NaCl, 87.5 mM mannitol, 12.5 mM Tris-Hepes (pH 7) and 2.5 mM EDTA were eluted through a cation exchange resin with 175 mM mannitol, 5 mM Tris-Hepes (pH 7) to remove external  $\text{Na}^+$ . Before adding trace quantity of  $^{22}\text{Na}^+$  (initial  $[^{22}\text{Na}^+]_{\text{Ext}} = 20 \text{ nM}$ ), external osmolarity was adjusted with mannitol. Each point indicates mean  $^{22}\text{Na}^+$  uptake  $\pm$  S.E. at 60 min ( $n = 4-6$ ). Uptake is expressed as percent of total radioactivity per mg of membrane protein. The line, determined by linear regression analysis, has a correlation coefficient of 0.93. The effect of detergent Triton X-100 (0.5%) upon  $^{22}\text{Na}$  uptake after 60 min is also indicated.

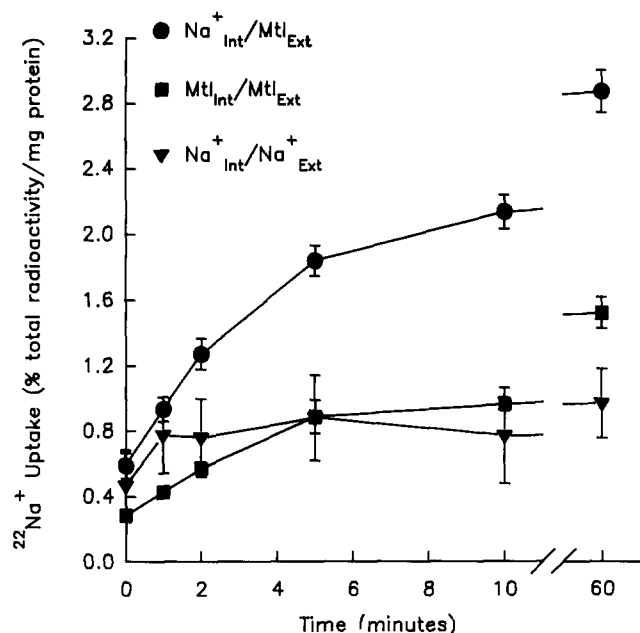


Fig. 3.  $^{22}\text{Na}^+$  accumulation by apical vesicles in the presence and absence of imposed transmembrane diffusion potentials.  $\text{Na}^+$ -loaded vesicles ( $\text{Na}_{\text{Int}}^+$ ) were prepared in 55 mM NaCl, 87.5 mM mannitol, 12.5 mM Tris-Hepes (pH 7) and 2.5 mM EDTA. Mannitol-loaded vesicles ( $\text{Mtl}_{\text{Int}}$ ) were prepared in 175 mM mannitol and 5 mM Tris-Hepes (pH 7). Vesicles were briefly incubated in 175 mM mannitol and 5 mM Tris-Hepes (pH 7) ( $\text{Mtl}_{\text{Ext}}$ ) or 5 mM NaCl, 87.5 mM mannitol and 5 mM Tris-Hepes (pH 7) ( $\text{Na}_{\text{Ext}}^+$ ) before adding trace  $^{22}\text{Na}^+$ . Incubation of  $\text{Na}^+$ -loaded vesicles in  $\text{Na}^+$ -free, mannitol medium ( $\text{Na}_{\text{Int}}^+/\text{Mtl}_{\text{Ext}}$ ; ●) imposed interior-negative transmembrane diffusion potentials. Incubation of  $\text{Na}^+$ -loaded vesicles in  $\text{Na}^+$  medium ( $\text{Na}_{\text{Int}}^+/\text{Na}_{\text{Ext}}^+$ ; ▼) or of mannitol-loaded vesicles in mannitol medium ( $\text{Mtl}_{\text{Int}}/\text{Mtl}_{\text{Ext}}$ ; ■) inhibited diffusion potential development. Each point indicates mean  $^{22}\text{Na}^+$  uptake  $\pm$  S.E. ( $n = 5-8$ ).

Over the next 23 h,  $^{22}\text{Na}^+$  uptake decreased by 38% to values observed at 2–5 min. Promotion and overshoot of uptake by interior-negative membrane potentials indicated the presence of electrogenic  $\text{Na}^+$  transport. Elimination of the promotional potential gradient (without removal of the externally directed  $\text{Na}^+$  gradient) by substitution of NaCl for external mannitol ( $\text{Na}_{\text{Int}}^+/\text{Na}_{\text{Ext}}^+$ ) reduced total uptake 66% ( $P < 0.01$ ) in the presence of a membrane-bound component and 97% ( $P < 0.01$ ) in its absence. Elimination of both the potential gradient and the unfavorable externally directed  $\text{Na}^+$  gradient by replacement of internal NaCl with mannitol ( $\text{Mtl}_{\text{Int}}/\text{Mtl}_{\text{Ext}}$ ) reduced inhibition of  $^{22}\text{Na}^+$  uptake to 47% ( $P < 0.01$ ) – 68% after subtracting the membrane-bound component ( $P < 0.01$ ; Fig. 3). This persistent  $\text{Na}^+$  uptake by mannitol-loaded vesicles in the absence of a transmembrane potential gradient suggested an alternative nonelectrogenic path of  $^{22}\text{Na}^+$  uptake, possibly via  $\text{H}^+$  coupling.

#### Evidence for sodium/proton exchange across apical membranes

Total  $^{22}\text{Na}^+$  uptake was reassessed in the presence of known cationic substitutes ( $\text{H}^+$  and  $\text{NH}_4^+$ ) for  $\text{Na}^+$

during  $\text{Na}^+/\text{H}^+$  exchange. Studies were conducted in the presence of induced transmembrane diffusion potentials for two reasons: (1) concurrent electrogenic  $\text{Na}^+$  uptake increased assay sensitivity to non-membrane-bound  $^{22}\text{Na}^+$  uptake by reducing the relative contribution of membrane-bound  $^{22}\text{Na}^+$  to total  $^{22}\text{Na}^+$  uptake and (2) interior-negative membrane potentials promoted internal acidification, thus favoring  $^{22}\text{Na}^+$  uptake by  $\text{Na}^+/\text{H}^+$  exchange. Internally-directed  $\text{H}^+$  and  $\text{NH}_4^+$  gradients individually inhibited total  $\text{Na}^+$  uptake (Fig. 4). External  $\text{H}^+$  (pH 6) reduced  $^{22}\text{Na}^+$  uptake 40% ( $P < 0.0001$ ), and external  $\text{NH}_4^+$  (10 mM) reduced  $^{22}\text{Na}^+$  uptake 48% ( $P < 0.001$ ). These observations of reduced  $^{22}\text{Na}^+$  uptake suggested decreased  $\text{Na}^+/\text{H}^+$  exchange activity despite concurrent  $\text{Na}^+$  conductance.

To assess  $\text{H}^+$  movement during proposed  $\text{Na}^+/\text{H}^+$  exchange, change in transmembrane pH gradient was monitored by absorbance change associated with AO trapping. Internal alkalization of mannitol-loaded vesicles was investigated in the presence and absence of externally directed  $\text{H}^+$  gradients.  $\text{Na}^+$ -loaded vesicles with transmembrane diffusion potentials were not systematically investigated because of increased internal trapping of cationic AO in early experiments. In the presence of externally directed proton gradients, alkalization was promoted by external  $\text{Na}^+$  ( $\text{Mtl}(\text{pH } 6)_{\text{Int}}/\text{Na}^+(\text{pH } 7)_{\text{Ext}}$ ) (Fig. 5). Absence of external  $\text{Na}^+$  minimized proton efflux in the same ionic environment

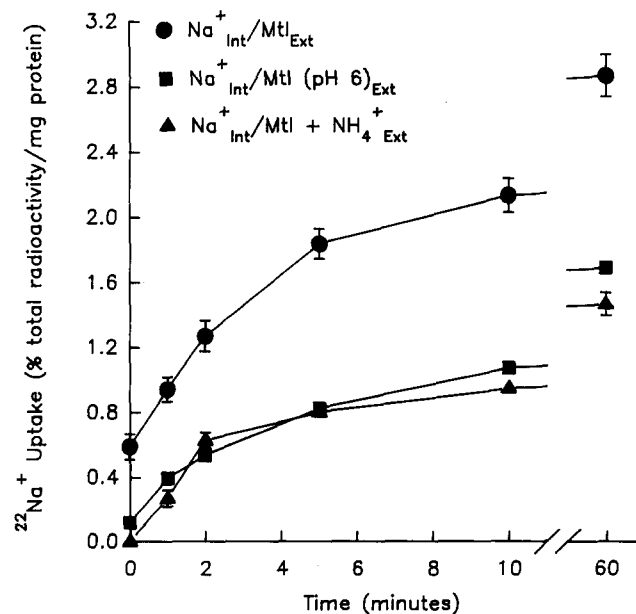


Fig. 4. Effect of  $\text{Na}^+/\text{H}^+$  exchange inhibitors upon  $^{22}\text{Na}^+$  accumulation.  $\text{Na}^+$ -loaded vesicles were incubated in mannitol medium in the presence of  $\text{Na}^+/\text{H}^+$  exchange inhibitors  $\text{H}^+$  (pH 6) ( $\text{Na}_{\text{Int}}^+/\text{Mtl}(\text{pH } 6)_{\text{Ext}}$ ; ■) and 10 mM  $\text{NH}_4^+$  ( $\text{Na}_{\text{Int}}^+/\text{Mtl} + \text{NH}_4^+_{\text{Ext}}$ ; ▲). Uptake in the absence of  $\text{Na}^+/\text{H}^+$  exchange inhibitors are included ( $\text{Na}_{\text{Int}}^+/\text{Mtl}_{\text{Ext}}$ ; ●). Each point indicates mean  $^{22}\text{Na}^+$  uptake  $\pm$  S.E. ( $n = 4-8$ ).

((Mtl(pH 6)<sub>Int</sub>/Mtl(pH 7)<sub>Ext</sub>). In the absence of an imposed externally-directed H<sup>+</sup> gradient, spontaneous internal acidification occurred that was succeeded by alkalization only in the presence of external Na<sup>+</sup>(Mtl(pH 7)<sub>Int</sub>/Na<sup>+</sup>(pH 7)<sub>Ext</sub>).

#### Amiloride inhibition of sodium uptake and proton efflux

Amiloride-sensitive <sup>22</sup>Na<sup>+</sup> uptake was observed under electrogenic conditions (Na<sup>+</sup><sub>Int</sub>/Mtl<sub>Ext</sub>) (Fig. 6). Amiloride concentration of 0.1 mM was employed based on cited inhibitory concentrations during investigation of Na<sup>+</sup> uptake by intact pneumocytes. Amiloride alone inhibited Na<sup>+</sup> uptake by apical vesicles 52% (*P* < 0.01). Combination of NH<sub>4</sub><sup>+</sup> with amiloride or of H<sup>+</sup> (external pH 6) with amiloride increased observed inhibition to 61% (*P* < 0.005). By contrast, furosemide (1 mM), an inhibitor of electroneutral Na<sup>+</sup>/Cl<sup>-</sup> co-transport, did not influence uptake (Fig. 6).

Amiloride-sensitive <sup>22</sup>Na<sup>+</sup> uptake was reinvestigated at 30 min over a range of amiloride concentrations. Limited amiloride solubility restricted maximal concentrations to 1 mM. A dose-effect curve (Fig. 7) constructed over a range of 1–1000 μM indicated the median effective dose at approx. 100 μM. At the low

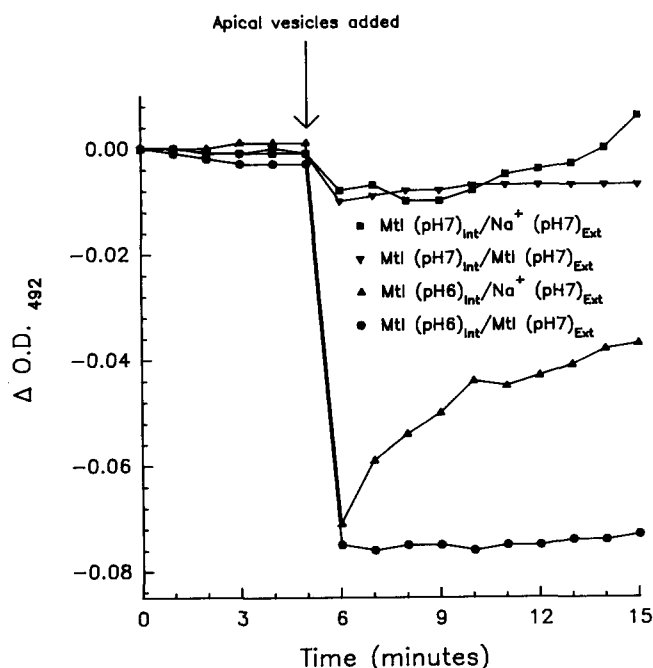


Fig. 5. Effect of external Na<sup>+</sup> upon proton efflux in the absence of imposed transmembrane diffusion potentials. At time zero, prewarmed 55 mM NaCl, 87.5 mM mannitol with 5 mM Tris-Hepes (pH 7) (Na<sup>+</sup>(pH 7)<sub>Ext</sub>) or 175 mM mannitol with 5 mM Tris-Hepes (pH 7) (Mtl(pH 7)<sub>Ext</sub>) was added to 6 μM Acridine orange in a thermostatted cuvette (37°C). At 5 min, prewarmed apical vesicles loaded with 175 mM mannitol and 5 mM Tris-Hepes (pH 6 or 7) (Mtl(pH 6)<sub>Int</sub> or Mtl(pH 7)<sub>Int</sub>) were added. Differences in absorbance at 492 nm (ΔA<sub>492 nm</sub>) between time zero and subsequent timepoints reflect the addition of vesicles and the redistribution of dye between intra- and extravascular spaces in response to changes in the transmembrane pH gradient.

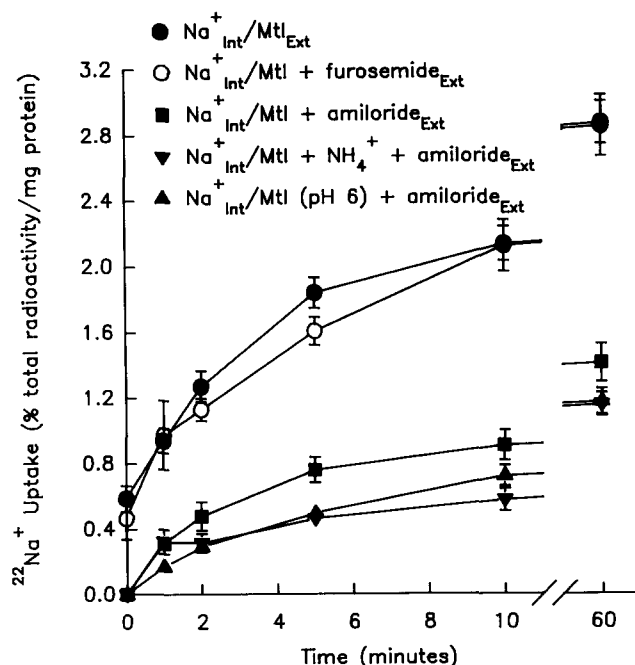


Fig. 6. Effect of amiloride, specific Na<sup>+</sup>/H<sup>+</sup> exchange inhibitors and furosemide upon <sup>22</sup>Na<sup>+</sup> uptake by apical vesicles. Na<sup>+</sup>-loaded vesicles were incubated in mannitol medium in the presence of 0.1 mM amiloride in the absence (Na<sup>+</sup><sub>Int</sub>/Mtl + amiloride<sub>Ext</sub>; ■) or presence of Na<sup>+</sup>/H<sup>+</sup> exchange inhibitors H<sup>+</sup> (pH 6) (Na<sup>+</sup><sub>Int</sub>/Mtl(pH 6) + amiloride<sub>Ext</sub>; ▲) or 10 mM NH<sub>4</sub><sup>+</sup> (Na<sup>+</sup><sub>Int</sub>/Mtl + NH<sub>4</sub><sup>+</sup> + amiloride<sub>Ext</sub>; ▼). Uptake in the presence of 1 mM furosemide (Na<sup>+</sup><sub>Int</sub>/Mtl + furosemide<sub>Ext</sub>; ○) or absence of additives (Na<sup>+</sup><sub>Int</sub>/Mtl<sub>Ext</sub>; ●) are included. Each point indicates mean <sup>22</sup>Na<sup>+</sup> uptake ± S.E. (*n* = 4–8).

end of the concentration range, 1 μM amiloride inhibited 10% of the observed amiloride-sensitive Na<sup>+</sup> uptake.

Amiloride also inhibited H<sup>+</sup> efflux under conditions previously associated with internal alkalization. In the presence or absence of imposed pH gradients, amiloride (0.1 mM) reduced observed proton effluxes (Fig. 8).

## Discussion

### Isolation of plasma membrane vesicles

A new method for isolation of plasma membrane vesicles from TIIP was developed to provide both apical and basolateral membrane populations of sufficient quantity and enrichment. Initially, the method was planned along lines of those that had been applied to tracheal epithelial cells [14]. However, this approach required several modifications because of the heterogeneous cell populations that line lower airways. Separation of individual cells from underlying connective tissues rendered cell homogenization by mechanical methods ineffective. Homogenization by nitrogen-bomb cavitation proved more effective than osmotic lysis. Continuous sucrose gradients provided better enrichment of plasma membrane fractions than discontinu-

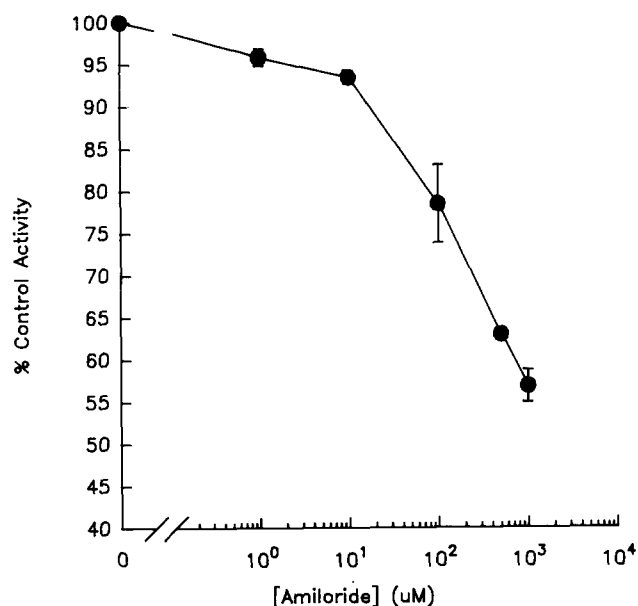


Fig. 7. Effect of different amiloride concentrations upon  $^{22}\text{Na}^+$  uptake by apical vesicles in the presence of interior-negative transmembrane diffusion potentials.  $\text{Na}^+$ -loaded vesicles (internal pH 7) were incubated in 175 mM mannitol, 5 mM Tris-Hepes (pH 7) and amiloride at concentrations ranging from 1–1000  $\mu\text{M}$ .  $^{22}\text{Na}^+$  uptake were measured 30 min after addition of trace  $^{22}\text{Na}^+$ . Each point indicates the mean  $^{22}\text{Na}^+$  uptake  $\pm$  S.E. expressed as a percentage of mean  $^{22}\text{Na}^+$  uptake in the absence of added amiloride (control uptake) ( $n = 5$  or 6).

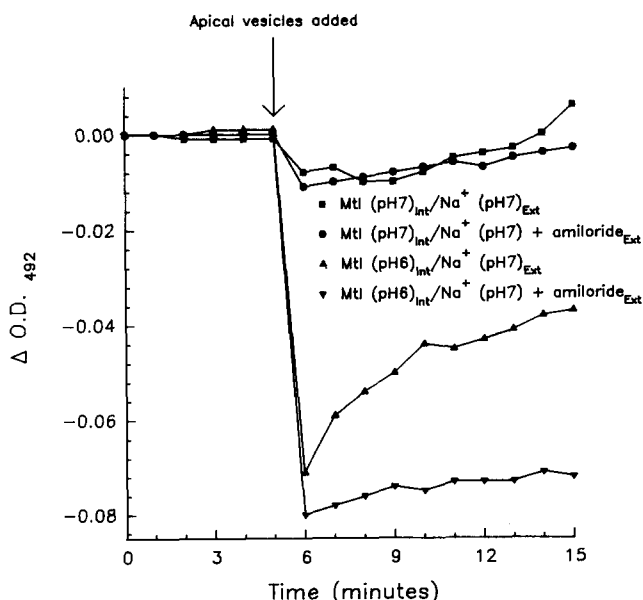


Fig. 8. Effect of amiloride upon proton efflux from apical vesicles. At time zero, prewarmed 55 mM NaCl, 87.5 mM mannitol and 5 mM Tris-Hepes (pH 7) without ( $\text{Na}^+$  (pH 7)<sub>Ext</sub>) or with 0.1 mM amiloride ( $\text{Na}^+$  (pH 7) + amiloride<sub>Ext</sub>) was added to 6  $\mu\text{M}$  acridine orange in a thermostatted cuvette (37°C). At 5 min, prewarmed apical vesicles loaded with 175 mM mannitol and 5 mM Tris-Hepes (pH 6 or 7) (Mtl(pH 6)<sub>int</sub> or Mtl(pH 7)<sub>int</sub>) were added. Differences in absorbance at 492 nm ( $\Delta A_{492\text{ nm}}$ ) between time zero and subsequent timepoints reflect the addition of vesicles and changes in the transmembrane pH gradient.

ous sucrose gradients or differential centrifugation. Incubation of mixed plasma membrane fractions with  $\text{Mg}^{2+}$  (10 mM) improved apical membrane purification slightly [22]. But the small improvement did not offset the reported risks of reducing net yields and altering vesicular transport properties [23–26].

By comparison with other preparations of epithelial membrane vesicles, the current method provides significantly enriched apical and basolateral plasma membrane fractions with minimal contamination by other organelles. Apical vesicles are enriched 5-fold in the alkaline phosphatase marker with less than 2-fold enrichment of the other enzyme markers, including  $\text{Na}^+, \text{K}^+$ -ATPase (1.7-fold enrichment). Alkaline phosphatase enrichment is intermediate between those of other reported preparations of TIIP apical membranes (1.8- and 18–24-fold enrichments) [10,11]. Contamination of the apical fraction by  $\text{Na}^+, \text{K}^+$ -ATPase is 2-fold less than that of the other reported preparations. Previous efforts to isolate basolateral vesicles have not been reported. In the current investigation, basolateral vesicles are enriched 23-fold in the  $\text{Na}^+, \text{K}^+$ -ATPase marker with less than 2-fold enrichment of alkaline phosphatase (1.9-fold) and less than 1-fold enrichment of the other enzyme markers.

#### $^{22}\text{Na}$ and proton transport by apical membrane vesicles

Widespread investigations of sodium transport by cell suspensions, confluent monolayers, or plasma membrane vesicles of TIIPs support the presence of at least three different sodium transport activities. In the absence of distinguishable cell polarity, cells suspended in media demonstrate: (1) ouabain-sensitive  $\text{Na}^+, \text{K}^+$ -ATPase activity [5] and (2) amiloride-sensitive, electroneutral  $\text{Na}^+/\text{H}^+$  exchange [8]. Investigations of confluent monolayers localize the ouabain-sensitive  $\text{Na}^+, \text{K}^+$ -ATPase to the basolateral membrane. They also identify a third source of  $\text{Na}^+$  transport at the apical membrane – electrogenic, amiloride-sensitive  $\text{Na}^+$  conductance [1,3,4].

Investigations of  $\text{Na}^+$  transport by plasma membrane vesicles reexamine the question of amiloride-sensitive  $\text{Na}^+$  transport at the apical membrane. Employing apical membranes of fetal sheep pneumocytes, Butcher et al. conclude that insensitivity to amiloride at concentrations less than 1 mM is most consistent with amiloride-sensitive  $\text{Na}^+/\text{H}^+$  exchange [9]. Shaw et al. extend these observations to include promotion of  $\text{Na}^+$  uptake by outwardly-directed proton gradients [10]. By contrast, Matalon et al., employing apical vesicles from adult rabbit lungs, conclude that observed  $\text{Na}^+$  uptake is consistent with  $\text{Na}^+$  conductance and inconsistent with  $\text{Na}^+/\text{H}^+$  exchange because of decreased  $\text{Na}^+$  uptake in the presence of outwardly-directed  $\text{H}^+$  gradients [11].

The present study of  $\text{Na}^+$  uptake by the apical



membranes of mature TIIPs provides evidence of both  $\text{Na}^+$  conductance and  $\text{Na}^+/\text{H}^+$  exchange at the alveolar side of pneumocytes. The possibility of influential  $\text{Na}^+/\text{K}^+$ -ATPase activity is eliminated by exclusion of ATP from experimental conditions and by absence of demonstrable enzyme activity in thawed vesicles.  $^{22}\text{Na}^+$  uptake into an osmotically-active space is demonstrated by the linear inverse relationship between uptake and extravesicular osmolarity. Extrapolation of uptake to infinite osmolarity and uptake in the presence of detergent suggest that 25–30% of uptake occurs by membrane binding. This figure compares favorably with the binding estimates for other TIIP apical membrane preparations (48–49% binding) [9,11].

Evidence for electrogenic  $\text{Na}^+$  conductance is provided by: (1) promotion and overshoot of  $^{22}\text{Na}^+$  uptake by interior-negative diffusion potentials; (2) persistent sensitivity to amiloride after blockade of  $\text{Na}^+/\text{H}^+$  exchange by internally directed  $\text{H}^+$  or  $\text{NH}_4^+$  gradients; and (3) sensitivity to amiloride at 1  $\mu\text{M}$  concentration.  $^{22}\text{Na}^+$  uptake is initially investigated under conditions favoring electrogenic transport. Creation of outwardly-directed cation ( $\text{Na}^+$ ) gradients establishes transient diffusion potentials across the membranes of vesicles permeable for the cation ( $\text{Na}^+$ ) of interest [19]. This method provides greater simplicity and better selectivity for  $\text{Na}^+$  cations than exposure of  $\text{K}^+$ -loaded vesicles to valinomycin – an alternative method for imposing interior-negative diffusion potentials. Uptake is maximal in the presence of  $\text{Na}^+$  diffusion potentials ( $\text{Na}_{\text{Int}}^+/\text{Mtl}_{\text{Ext}}^+$ ; Fig. 3). Both the observed time-course over 60 min and the pattern of uptake are nearly identical to those observed for fetal sheep and adult rabbit TIIP apical membranes [9,11]. Removal of the diffusion potential reduces uptake approx. 65% in the presence of a shallow, inwardly-directed  $\text{Na}^+$  gradient ( $\text{Mtl}_{\text{Int}}/\text{Mtl}_{\text{Ext}}$ ). Removal of both diffusion potential and  $\text{Na}^+$  gradient reduces uptake 97% ( $\text{Na}_{\text{Int}}^+/\text{Na}_{\text{Ext}}^+$ ). Overshoot is characteristic of electrogenic  $\text{Na}^+$  uptake by epithelial plasma membrane vesicles [19,27]. In this study, delayed dissipation of the potential gradient occurs after the initial 60 min study period. The pattern of overshoot is similar to that observed by Mat-alon et al. employing apical TIIP vesicles with valinomycin-induced diffusion potentials [11].

Uptake sensitivity to amiloride is observed over a concentration range of 1–1000  $\mu\text{M}$  (Fig. 7). The shape, median effective inhibitory dose and maximally observed inhibition are similar to dose-response curves constructed for  $\text{Na}^+$  conductances in toad bladder and rabbit lung membrane vesicles [11,27]. Median effective inhibitory doses range between 10–100  $\mu\text{M}$  in the three studies. Maximal percent inhibitions are 45–65%. The possibility of multiple amiloride-sensitive  $\text{Na}^+$  transport mechanisms complicates the interpretation of these sensitivity data. In addition to at least two dis-

tinct populations of amiloride-sensitive  $\text{Na}^+$  channels, the first with high affinity for amiloride ( $< 1 \mu\text{M}$ ) and the second with lower affinity ( $< 200 \mu\text{M}$ ), electroneutral  $\text{Na}^+/\text{H}^+$  exchange and electrogenic  $\text{Na}^+/\text{Ca}^{2+}$  exchange are amiloride-sensitive at concentrations of 3–100  $\mu\text{M}$  and 1 mM, respectively [27,28]. To distinguish between amiloride-sensitive  $\text{Na}^+$  uptake by  $\text{Na}^+$  conductance and  $\text{Na}^+/\text{H}^+$  exchange,  $\text{Na}^+$  uptake in the present study is reexamined in the presence of amiloride and presence or absence of  $\text{Na}^+/\text{H}^+$  blockade by internally directed  $\text{H}^+$  gradients (Fig. 6). Amiloride (0.1 mM) inhibits  $\text{Na}^+$  uptake 77% (after subtracting the membrane-bound  $^{22}\text{Na}^+$ ) in the absence of imposed proton gradients ( $\text{Na}_{\text{Int}}^+/\text{Mtl} + \text{amiloride}_{\text{Ext}}$ ). In the presence of proton gradients (external pH values  $\leq 6$ ) that cause complete  $\text{Na}^+/\text{H}^+$  blockade in other epithelia [29], amiloride inhibits  $\text{Na}^+$  uptake by  $\text{Na}^+$  conductance an additional 14% ( $\text{Na}_{\text{Int}}^+/\text{Mtl}(\text{pH } 6) + \text{amiloride}_{\text{Ext}}$ ).

Lastly, the demonstration of amiloride inhibition at doses as low as 1  $\mu\text{M}$  confirms amiloride-sensitive sodium conductance (Fig. 7). Although the observed median effective inhibitory dose of approx. 100  $\mu\text{M}$  is greater than that expected in the presence of substantial  $\text{Na}^+$ -conductance activity, similar shifts in the dose-response curves of other epithelia are attributed to  $\text{Na}^+$  conductances with high and low affinities for amiloride [27,28]. The possibility of two different  $\text{Na}^+$  conductances at the apical membrane of TIIPs have been suggested [11].

Other pathways of electrogenic  $\text{Na}^+$  transport occur in polarized epithelia. These include  $\text{Na}^+/\text{Ca}^{2+}$  exchange and  $\text{Na}^+$ -coupled glucose or amino-acid transport. The possibility of observing either of these other transporters is eliminated in these studies by the exclusion of supplemental  $\text{Ca}^{2+}$ , glucose and amino acids from the media; chelation of residual  $\text{Ca}^{2+}$  with EDTA; and restriction of amiloride availability to concentrations 10- to 20-fold less than those necessary for inhibition of  $\text{Na}^+/\text{Ca}^{2+}$  exchange or  $\text{Na}^+$ -coupled glucose transport.

Several lines of evidence indicate the presence of  $\text{Na}^+/\text{H}^+$  exchange at the apical membranes of TIIPs. Although prior investigations of apical plasma membrane vesicles conflict with regard to presence of  $\text{Na}^+/\text{H}^+$  exchange, identification of  $\text{Na}^+/\text{H}^+$  exchange in TIIP cell suspensions is well-documented [8]. The current study demonstrates electrically-neutral coupling of  $\text{Na}^+$  and  $\text{H}^+$  exchange at the apical membrane by: (1) presence of electrically-neutral,  $\text{Na}^+$ -dependent internal alkalinization; (2) inhibition of  $\text{Na}^+$  uptake by internally-directed  $\text{H}^+$  and  $\text{NH}_4^+$  gradients; (3) presence of electrically-neutral  $\text{Na}^+$  uptake with a similar time-course to internal alkalinization; and (4) inhibition of both  $\text{Na}^+$  uptake and internal alkalinization by amiloride.

Coupling of  $H^+$  efflux to  $Na^+$  uptake is most apparent for internally acidified, electrically-neutral, mannitol-loaded vesicles (Fig. 5,  $(Mtl(pH\ 6)_{Int}/Na^+(pH\ 7)_{Ext})$ ). A rapid change of absorbance in the presence of externally available  $Na^+$  is indicative of  $Na^+$ -dependent internal alkalinization. Absence of external  $Na^+$  is associated with minimal decay in pH gradient ( $Mtl(pH\ 6)_{Int}/Mtl(pH\ 7)_{Ext}$ ). By comparison, a delayed, more shallow change of absorbance occurs in the absence of internal acidification and presence of external  $Na^+$  ( $Mtl(pH\ 7)_{Int}/Na^+(pH\ 7)_{Ext}$ ). This delayed change may reflect spontaneous development of internally negative diffusion potentials [30], accompanied by internal acidification via passive  $H^+$  conductance into the negatively-charged intravesicular space [30–32]. The uptake of  $^{22}Na^+$  under similar conditions (Fig. 3,  $(Mtl_{Int}/Mtl_{Ext})$ ) might also occur by  $Na^+/H^+$  exchange after internal acidification of mannitol-loaded vesicles. Alternative contributions from  $Na^+/Na^+$  exchange have not been excluded.

Additional support for coupling between  $Na^+$  uptake and  $H^+$  efflux comes from known inhibitors of  $Na^+/H^+$  exchange and comparison of  $^{22}Na^+$  uptake and vesicle alkalinization over time.  $^{22}Na^+$  uptake is significantly inhibited by internally-directed  $H^+$  and  $NH_4^+$  gradients (Fig. 4) [29]. Amiloride (0.1 mM) inhibits  $Na^+$ -dependent alkalinization of vesicles (Fig. 8), as well as, the pH-sensitive component of  $^{22}Na^+$  uptake (Fig. 6). Lastly,  $^{22}Na^+$  uptake by mannitol-loaded vesicles (Fig. 3) and alkalinization of acidified vesicles in the presence of external  $Na^+$  (Fig. 5) both plateau within about 10 min.

Plasma membrane vesicles constitute one of the simplest systems with which to investigate transport processes. The present method describes a means of separating apical from basolateral plasma membrane vesicles in TIIP preparations. In initial investigations with apically-derived vesicles, evidence is provided for coexistence of  $Na^+$  conductance channels and  $Na^+/H^+$  exchangers at the apical membrane of mature TIIPs. The availability of apical and basolateral vesicle populations provides new opportunities to investigate transcellular transport activities between alveolar and interstitial compartments of the lung.

### Acknowledgements

The authors are grateful to Dr. William P. Dubinsky for invaluable discussions and helpful technical suggestions. This work was supported by National Heart, Lung and Blood Institute Grant HL-02292 and American Lung Association Research Grant 511-2-7274.

### References

- Goodman, B.E., Fleischer, R.S. and Crandall, E.D. (1983) *Am. J. Physiol.* 245, C78–C83.
- Olver, R.E., Schneeberger, E.E. and Walters, D.V. (1981) *J. Physiol.* 315, 395–412.
- Rao, A.K. and Cott, G.R. (1991) *Am. J. Physiol.* 261, L178–L187.
- Cott, G.R., Sugahara, K. and Mason, R.J. (1986) *Am. J. Physiol.* 250, C222–C227.
- Bland, R.D. and Boyd, C.A.R. (1986) *J. Appl. Physiol.* 61, 507–515.
- Kleyman, T.R. and Cragoe, E.J. (1988) *J. Membr. Biol.* 105, 1–21.
- Nielson, D.W. (1988) *Pediatr. Res.* 23, 418–422.
- Nord, E.P., Brown, S.E.S. and Crandall, E.D. (1987) *Am. J. Physiol.* 252, C490–C498.
- Butcher, P.A., Steele, L.W., Ward, M.R. and Olver, R.E. (1989) *Biochim. Biophys. Acta* 980, 50–55.
- Shaw, A.M., Steele, L.W., Butcher, P.A., Ward, M.R. and Olver, R.E. (1990) *Biochim. Biophys. Acta* 1028, 9–13.
- Matalon, S., Bridges, R.J. and Benos, D.J. (1991) *Am. J. Physiol.* 260, L90–L96.
- Augustin-Voss, H.G., Schoon, H.A., Stockhofe, N. and Uebesch, S. (1989) *Lung* 167, 1–10.
- Kikkawa, Y. and Yoneda, Y. (1974) *Lab. Invest.* 30, 76–84.
- Langridge-Smith, J.E., Field, M. and Dubinsky, W.P. (1983) *Biochim. Biophys. Acta* 731, 318–328.
- Norby, J.G. (1988) *Methods Enzymol.* 156, 116–119.
- Hochstadt, J., Quinlan, D.C., Rader, R.L., Chen-Chung, L. and Dowd, D. (1975) *Methods Membr. Biol.* 5, 117–162.
- LaBarca, C. and Paigen, K. (1980) *Anal. Biochem.* 102, 344–352.
- Lowry, O.H., Rosebrough, N.J., Farr, A.L. and Randall, R.J. (1951) *J. Biol. Chem.* 193, 265–275.
- Garty, H., Rudy, B. and Karlisch, S.J.D. (1983) *J. Biol. Chem.* 258, 13094–13099.
- Gasko, O.D., Knowles, A.F., Shertzer, H.G., Suolinna, E.M. and Racker, E. (1976) *Anal. Biochem.* 72, 57–65.
- Palmgren, M.G. (1991) *Anal. Biochem.* 192, 316–321.
- Aubry, H., Merrill, A.R. and Proulx, P. (1986) *Biochim. Biophys. Acta* 856, 610–614.
- Biber, J.B., Stieger, K., Haase, W. and Murer, H. (1981) *Biochim. Biophys. Acta* 647, 169–176.
- Bofta, G., Meyer, G., Rossetti, C. and Cremaschi, D. (1987) *Biochim. Biophys. Acta* 897, 315–323.
- Lipkowitz, M.S. and Abramson, R.G. (1987) *Am. J. Physiol.* 252, F700–F711.
- Sabolic, I. and Burkhardt, G. (1984) *Biochim. Biophys. Acta* 772, 140–148.
- Garty, H. (1984) *J. Membr. Biol.* 82, 269–279.
- Moran, A., Asher, C., Cragoe, E.J. and Garty, H. (1988) *J. Biol. Chem.* 263, 19586–19591.
- Aronson, P.S., Suhm, M.A. and Nee, J. (1983) *J. Biol. Chem.* 258, 6767–6771.
- Landridge-Smith, J.E. and Dubinsky, W.P. (1985) *Am. J. Physiol.* 249, C417–C420.
- Dudeja, P.K., Foster, E.S. and Brasitus, T.A. (1989) *Am. J. Physiol.* 257, G6242–G632.
- Meyer, G., Botta, G., Rossetti, C. and Cremaschi, D. (1990) *J. Membr. Biol.* 118, 107–120.